ACS APPLIED MATERIALS & INTERFACES

Research Article

www.acsami.org

# Novel Application of Polyelectrolyte Multilayers as Nanoscopic Closures with Hermetic Sealing

Stephanie A. Marcott,[†] Sena Ada,[‡] Phillip Gibson,[†] Terri A. Camesano,[‡] and R. Nagarajan*[,†]

[†]Molecular Sciences and Engineering Team, Natick Soldier Research, Development & Engineering Center, Natick, Massachusetts 01760, United States

[‡]Department of Chemical Engineering, Worcester Polytechnic Institute, Worcester, MA

**ABSTRACT:** Closure systems for personnel protection applications, such as protective clothing or respirator face seals, should provide effective permeation barrier to toxic gases. Currently available mechanical closure systems based on the hook and loop types (example, Velcro) do not provide adequate barrier to gas permeation. To achieve hermetic sealing, we propose a nonmechanical, nanoscopic molecular closure system based on complementary polyelectrolyte multilayers, one with a polycation outermost layer and the other with a polyanion outermost layer.

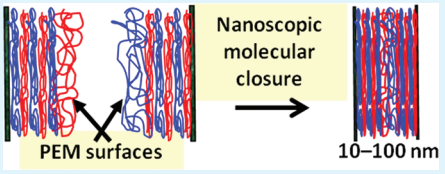


The closure surfaces were prepared by depositing polyelectrolyte multilayers under a variety of deposition conditions, on conformable polymer substrates (thin films of polyethylene teraphthalate, PET or polyimide, PI). The hermetic sealing property of the closures was evaluated by measuring the air flow resistance using the dynamic moisture permeation cell (DMPC) at different humidity conditions. The DMPC measurements show that the polyelectrolyte multilayer closures provide significantly large resistance to air flow, approximately 20−800 times larger than that possible with conventional hook and loop type closure systems, at all humidity levels (from 5 to 95% relative humidity). Hence, from the point of view of providing a hermetic seal against toxic gas permeation, the polyelectrolyte multilayer closures are viable candidates for further engineering development. However, the adhesive strength of the multilayer closures measured by atomic force microscopy suggests that the magnitude of adhesion is much smaller than what is possible with mechanical closures. Therefore, we envisage the development of a composite closure system combining the mechanical closure to provide strong adhesion and the multilayer closure to provide hermetic sealing.

**KEYWORDS:** *polyelectrolyte multilayer closures, dynamic moisture permeation cell, polyelectrolyte multilayers, adhesion between multilayer surfaces, multilayer deposition on flexible substrates, air flow resistance of multilayer closure, AFM colloidal probe force measurements, surface roughness of multilayers*

## INTRODUCTION

Mechanical closures such as Velcro are widely used in many applications. The mechanics of Velcro bonding is analogous to zippers and button snaps. Adhesion occurs by mechanical interlocking of two complementary mating interfaces, one with hooks and the other with loops. By applying sufficient pressure, the flexible microstructure on one interface is allowed to interlock with another flexible microstructure on the mating interface. Mechanical closures are capable of providing a wide range of adhesive bonding with very strong adhesion capabilities. However, mechanical closures with macroscopic contact roughness are critical sources of leaks in protective clothing/equipment, limiting the protective capability of the ensemble. This demands the invention of novel closure systems with good barrier properties that would retain the adhesion strength of the mechanical closures while enhancing the hermetic sealing.

Concepts for inventing novel nonmechanical closures can be derived from biological examples. It has been recognized that the ease of attachment and detachment on surfaces are controlled by the structure, size and shape of contact elements, and having a large number of small contact elements is favorable.[1−3] We propose in this paper that such surfaces with a large number of contact elements can be generated using polyelectrolyte (or other polymer) multilayers on both rigid and flexible substrates. The loops and tails of the adsorbed polyelectrolyte layers and the hydrophobic side chains (if any) on them serve as the numerous contact elements. Additional nanoscale contact elements can be created by building a layer of polyelectrolyte micelles as the outermost layer of the multilayer or by incorporating nanoparticles within the multilayer. We anticipate, as shown in Figure 1, that compared to the macroscopic gaps that exist in hook and loop type mechanical closures, the nonmechanical multilayer closure would mainly involve nanoscopic gaps, which will lead to a significant increase in their barrier properties.

Polyelectrolyte multilayer (PEM) films are prepared by layer-by-layer (LbL) assembly of alternately adsorbing positively and negatively charged ionic polymers onto a charged surface.[4] The simplicity of the process has led to significant research activity focused on the properties and potential applications of the multilayers, with more than 2900 entries appearing in the Web

Received: December 15, 2011
Accepted: March 5, 2012
Published: March 5, 2012

  

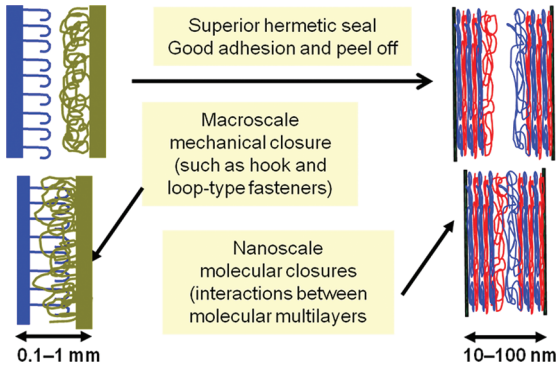


**Figure 1.** Schematic of polyelectrolyte multilayer (PEM) closure in comparison to mechanical hook and loop type closure. For Velcro type closure, the two closure surfaces are separated from one another at millimeter distances, whereas for the polymer multilayers, we anticipate separation distance in the nanometer range.

of Science search corresponding to the term "polyelectrolyte multilayer". Typically, the substrate is coated with a molecular layer of polycation (often polyethylene imine, PEI) by dipping in a cationic polyelectrolyte solution. This is then followed by the sequential dipping into an anionic polyelectrolyte solution and a cationic polyelectrolyte solution, a number of times depending on the number of polymer layers desired. In between the dipping steps, usually one incorporates the washing of coated surface with water to remove unadsorbed or poorly adsorbed polymer molecules. The formation of the multilayer by this dipping process is relatively slow (of the order of hours) and a more rapid production method based on spraying has also been reported in the literature[5−9] to reduce the process time to minutes. The dipping or spray process is carried out using polyelectrolyte solutions in which different counterions at varying concentrations may be present and which may have varying pH values. The solution properties of pH, ionic strength, type of electrolyte, the polyelectrolyte concentration, and the detailed process conditions all influence the nature of the multilayer formed.

Almost all of the studies on PEM in the literature have used rigid substrates such as silica, mica, quartz, glass, or polymer beads to deposit the multilayers, and only a handful of the papers[10,11] have reported the formation of the multilayers on conformable, flexible substrates. No systematic studies of polyelectrolyte multilayer formation on flexible polymer film substrates is currently available and all generalizations made in the literature regarding the multilayer formation process (growth mechanisms) and the multilayer properties (thickness, roughness, zeta potential as a function of formation variables) are based on multilayer deposition studies conducted on rigid substrates.[12] In the present work, we have deposited polyelectrolyte multilayers on flexible polymer films (polyethylene terephthalate, PET and polyimide, PI) and evaluated their potential as closure systems by measuring the air flow resistance of the closures at different humidity conditions, using the dynamic moisture permeation cell (DMPC) developed previously[13,14] at the Natick Soldier Center. The DMPC measurements show that the multilayer closures provide order of magnitude increase in the resistance to air permeation at all humidity levels when compared to the conventional hook and loop type closures.

Although the primary emphasis of this study is on the air flow resistance measurements, the other property of relevance to closure application is adhesion. Adhesion force measurements on polyelectrolyte multilayers deposited on rigid substrates have been reported in previous studies[15−20] mostly in liquid environments using atomic force microscopy (AFM) and surface force apparatus (SFA). The adhesive interactions derived from these nanoscale methods can provide qualitative information on the macroscopic adhesive properties of the multilayer closure. Claesson et al.[15] investigated the interactions in air between two-polyelectrolyte coated surfaces (not multilayers) and between a polyelectrolyte-coated surface and a bare surface using SFA and observed larger adhesion between a polyelectrolyte coated surface and a bare surface compared to that between two polyelectrolyte coated surfaces. Mermut et al[16] used AFM to carryout force−distance measurements in aqueous medium for the multilayer system, poly(allylamine hydrochloride) (PAH), and an azobenzene containing polyelectrolyte (P-Azo) prepared at varying charge densities. Between oppositely charged multilayer surfaces, adhesion values between 0.5 and 6.7 nN were found, with the highly ionically cross-linked samples exhibiting the largest adhesion. Bosio et al.[17] studied the interactions in aqueous medium between two identical polystyrene sulfonate (PSS)/PAH multilayer surfaces formed on both a colloidal silica probe and flat silica wafers, using AFM. Their results suggested that the interactions between symmetrical multilayer surfaces were repulsive and exhibited weak adhesion occasionally. Gong et al.[18] studied the interactions between a bare glass sphere and a glass substrate coated with PEMs formed from PSS/PAH and DNA/PAH, using AFM with a liquid cell. When PSS was deposited on the outermost layer, they did not observe any adhesion force between the glass sphere and the negatively charged PEM surface. They observed strong adhesion forces when PAH served as the outermost layer due to the interactions between the oppositely charged surfaces and possible entanglements of the polyelectrolyte chains that form a bridge between the glass particle and the multilayer. Notley et al.[19] measured the adhesive force between two multilayer covered silica surfaces. A decrease in the pull-off force was observed with the sequential adsorption of poly(acrylic acid) (PAA) after each PAH layer. They surmised that the higher pull-off force in the initial PAH layer, compared to the second PAH layer, is most probably due to the possibility of a bridging type adhesion interaction between the silica surfaces. With the subsequent adsorption of further polyelectrolyte layers, the possibility of bridging interactions is far lower due to the restricted availability of surface sites. Johansson et al.[20] investigated the adhesive interactions between two identical multilayers. In liquid cell, the AFM measurements showed a higher adhesion (pull-off force) when PAH was adsorbed in the outermost layers. A greater adhesion was observed for the low molecular weight polyelectrolytes. Furthermore, the adhesion increased with increasing contact time between the multilayers. The SFA adhesion measurements showed that under dry conditions, the adhesive forces between two high energetic mica substrates were actually lowered when they were covered by multilayers. It is evident that a number of variables including the polyelectrolyte molecular weight and concentration in solution, salt type and concentration in solution, the multilayer deposition process variables (dipping time, drying time), and the number of deposited bilayers can all affect the magnitude of the adhesion force measured.

In the present work, polyelectrolyte multilayers prepared under various solution conditions were imaged by atomic force

microscopy (AFM) to determine the surface roughness and adhesive force measurements between complementary multilayers (with oppositely charged surfaces) were made using colloidal probe AFM. On the basis of the results, we have concluded that the measured AFM adhesion force, when translated into macroscopic terms, is very small compared to that attainable with mechanical closures, implying that by itself, the polyelectrolyte multilayer closure will not be able to provide both the required adhesion and hermetic sealing. Indeed, macroscopic peel testing could not be performed on the multilayer closure using ASTM methods, since the peel strength is below the limit that can be measured. Therefore, the adhesion properties of the multilayers are not our continuing focus since we anticipate that a composite closure system will have to be engineered combining the mechanical closure to provide strong adhesion and the multilayer closure to provide mainly hermetic sealing.

## EXPERIMENTAL METHODS

**Materials.** Polyethylene terephthalate film (PET) and polyimide film (PI) were received from DuPont as Mylar LBT (48 gauge, 12 $\mu$m) and Kapton (3 mil, 75 $\mu$m), respectively, and were used as received to act as conformable, flexible substrates. The polyelectrolytes, polyethylene imine (PEI, molecular weight 6−10 × $10^5$), polyallylamine hydrochloride (PAH, molecular weight 7 × $10^4$), and polystyrene sulfonate (PSS, molecular weight 2 × $10^5$) were all purchased from Sigma Aldrich and made into 0.1% solutions with various salt concentrations and pH conditions. The sodium chloride (≥99.5% purity) was purchased from Sigma Aldrich; sodium fluoride (ACS grade), and sodium bromide (ACS grade) were purchased from Thomas Scientific. The pH adjustments were made dropwise with hydrochloric acid, 37% (1M) and sodium hydroxide, ≥98% (1M) purchased from Sigma Aldrich.

**Preparation of Polyelectrolyte Multilayers.** Polyelectrolyte multilayers were prepared on flexible polymer films as substrates. Prior to multilayer deposition, the polymer substrates (PET and PI) were air plasma-treated (PDC-32G, Harrick Plasma Cleaner) for 20 min to improve surface coverage and enhance adhesion between the substrate and the multilayer deposited on it. The layer-by-layer dipping technique was applied to prepare the polyelectrolyte multilayers. HMS$^{TM}$ Series Programmable Slide Container (Carl Zeiss, Inc.) was used for the dipping steps.

The preparation of multilayers was initiated by immersing the substrate into PEI solution followed by consecutive adsorption of oppositely charged polyelectrolytes PSS and PAH, from their solutions (30 min of dipping contact for each polyelectrolyte solution). The concentrations of the polyelectrolyte solutions were typically 0.1 wt %. Between each deposition step, the films were rinsed twice with water for 2 min each and dried in air for 10 min. The washing steps are helpful to remove the weakly adsorbed polymer molecules. The repetition of deposition of polyelectrolytes was continued until the desired number of layers was obtained.

For the investigation of effect of salt type, the polyelectrolyte solutions were prepared with NaF, NaCl, or NaBr at ionic strengths of 0.5 and 1.0 M. Given the slow process of multilayer preparation by the dipping method, more extensive changes in the preparation variables (such as more values of polyelectrolyte or salt concentrations, various drying and deposition times, etc) could not be pursued and the variables were selected mainly to identify any gross variations in the property of the closure system.

The designation PEI-($PSS_5PAH_5$) indicates a polyelectrolyte multilayer film deposited on the polymer substrate with PEI as the anchoring layer and five alternating layers of PSS and PAH, with cationic PAH as the outermost layer. The designation PEI-($PSS_6PAH_5$) indicates a polyelectrolyte multilayer film deposited on the polymer substrate with PEI as the anchoring layer and five alternating layers of PSS and PAH, with the sixth anionic PSS layer as the outermost. For all closure experiments, the complementary multilayers used were both formed on either PET or PI, and the two differing substrates were not used to create a closure together.

**Atomic Force Microscopy (AFM) Measurements of Surface Roughness.** Images of the polyelectrolyte multilayers were obtained using tapping mode atomic force microscopy. Regular silicon cantilevers (Asylum Research, manufacturer Olympus) with a spring constant of 42 N/m were used for imaging of the multilayers. The scan rate was kept constant at 1.0 Hz. A high resolution of 512 × 512 data

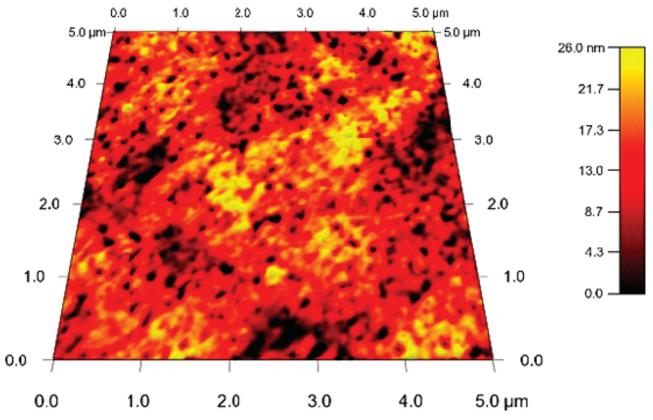


**Figure 2.** Surface roughness image of the multilayer PEI($PSS_5PAH_5$) prepared with 0.5 M NaBr. The colors indicate the scale of AFM height profiles. The rms roughness corresponding to this image is 6.51 nm.

points was acquired. A typical image is shown in Figure 2 for a multilayer with five bilayers. Roughness estimates were obtained using the AFM software. After acquiring the image (scan size of 5 $\mu$m), the image was flattened, a square box in dimensions of 1 $\mu$m x1 $\mu$m was created and the image was analyzed by carrying this box to different spots. The roughness was analyzed on at least two independent samples with 5 equally divided areas on each (having the number of measurements to be at least 10). The root-mean-square (rms) roughness values of the polyelectrolyte multilayers was calculated using the Igor Pro 6 software, according to, rms = $(\sum Y_i^2/N)^{1/2}$, where $Y_i$ is the height value and $N$ is the number of points (roughly 1 × $10^4$) for which the height measurements are made in the defined area. The roughness values measured at the 10 areas on the film were averaged to provide the tabulated results along with the standard deviation values. The rms roughness results depended on the analyzed area of the image; decreasing the analyzed area resulted in smaller rms roughness values.

**Atomic Force Microscopy Measurements of Adhesion Force.** AFM was also used to obtain the force−distance curve for the polymer multilayer surface interacting with the AFM probe and from the data, the pull-off force or a microscopic adhesion force is obtained. By this technique, the interactions between a bare or modified spherical colloidal probe and a planar multilayer surface can be measured and rough estimates of the adhesion strength between two complementary multilayers can be generated. For investigating the adhesion properties of the polyelectrolyte multilayers, three different types of AFM probes were used. Colloidal silica probes (1 $\mu$m $SiO_2$ particles) with a spring constant of 14 N/m were purchased from Novascan Technologies, Inc. in two forms: bare and functionalized with COOH surface chemistry. The third type of probe was prepared at our laboratory using the layer-by-layer deposition method − the bare silica probe was coated with a monolayer of PEI followed by a monolayer of PSS by manually dipping the probe into the solutions. The rinsing and drying steps were applied as well, in between the two depositions. The spring constant of this polyelectrolyte coated probe was assumed to be the same as bare colloidal silica probes. The probes were cleaned prior to AFM measurements leaving under UV light overnight. AFM, NanoScope IIIa (Dimension 3100, Veeco Metrology

Inc., Santa Barbara, CA), was used for the quantification of adhesion forces. Twenty-five force measurements were collected for each sample in air at ~45% relative humidity (RH) where the capillary force effects are not important. The cantilever was moved to five or ten different locations on the sample in both x and y directions, and five measurements were collected from each location. The raw force curves were processed with the assistance of self-written MATLAB and Microsoft Excel scripts.

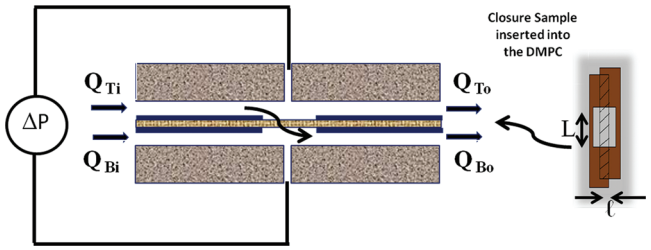


**Figure 3.** Schematic of the dynamic moisture permeation cell (DMPC) designed to measure the convection/diffusion transport of moisture and airflow resistance experiments under constant humidity conditions. The closure sample is inserted between the two compartments across which a pressure difference is maintained to drive air flow through the closure. The figure on the right shows the top down view of how the two multilayers are overlapped to create the closure that is inserted into the cell. The two multilayer strips are overlapped over the distance $l$, across which the pressure differential is applied. The flow area is bounded by the space $\delta$ between the two strips and the length $L$.

**Air Permeation Measurement with DMPC.** The dynamic moisture permeation cell (DMPC), shown in Figure 3, was designed to allow simultaneous measurements of air permeation and water vapor permeation through textile materials from a single experiment.[13,14] Both diffusive and convective transport of water vapor along with air permeation rates could be measured using this cell. In this study, only air permeation through closures is measured at different constant relative humidity levels. The cell consists of two compartments separated by the closure sample. Complementary polymer multilayers were deposited on either PET or PI polymer substrates (strips of size 0.025 m × 0.125 m) and the strips were hand pressed in air and overlapped by 0.0125 m to create the closure sample inside the DMPC where the pressure inputs are located (Figure 3). No load was applied on the closure area and within the DMPC cell opening, the closure is held taut by the top and bottom cell clamping plates. The closure was generated under dry conditions. For all closure experiments, the two complementary multilayers constituting the closure were deposited on identical substrate films, either PET or PI. The air pressure differences across textile layers due to factors such as wind or body motion have been estimated[13] to be less than 100 Pa. Because the closure design focused on personnel protection use has to withstand this range of pressure differential, the air permeation experiments in this study were done in this range of $\Delta P$ (pressure difference between the top and the bottom compartments). The volumetric air flow rate $Q$ across the closure sample as a function of the pressure differential $\Delta P$ provides a measure of the barrier properties of the closure.

Air streams of controlled relative humidity (generated by mixing dry air and air saturated with water vapor) are passed over the top and bottom surfaces of the sample, with the inlet volumetric flow rates at the top and the bottom denoted by $Q_{Ti}$ and $Q_{Bi}$. These inlet air flow rates are kept constant in the experiments at around 2000 $cm^3$/min (ref 13 provides detailed rationalizations for the conditions of operation of the DMPC). The outlet flow rates from the top and bottom compartments are denoted by $Q_{To}$ and $Q_{Bo}$. When $\Delta P = 0$, there is no driving force for flow across the closure. For this condition, no air flow can occur across the closure and the outlet flow rate $Q_{Bo}$ is simply equal to the inlet flow rate $Q_{Bi}$. For positive $\Delta P$, convective airflow across the closure occurs from the top to the bottom compartment. Therefore, the outlet flow rate $Q_{Bo}$ will be larger than the inlet flow rate $Q_{Bi}$. For negative $\Delta P$, convective airflow across the closure occurs from the bottom to the top compartment. Therefore, the outlet flow rate $Q_{Bo}$ will be smaller than the inlet flow rate $Q_{Bi}$. The flow rate $Q$ across the barrier is thus the difference between the outlet flow rate $Q_{Bo}$ and the inlet flow rate $Q_{Bi}$ at any $\Delta P$.

The relation between the volumetric flow rate of air through the barrier for a given applied pressure differential driving the flow is given by the phenomenological Darcy's law. The permeability constant $k_D$ of the barrier material is defined by the relation

$$k_D = \frac{\left(\frac{Q}{A}\right)\mu}{\left(-\frac{\partial P}{\partial Z}\right)}$$

where the pressure gradient $(-\partial P \partial Z)$ is the driving force for the air flow, $Q$ is the resulting volumetric flow rate of air through the barrier, $A$ is the cross-sectional area over which air flow occurs, and $\mu$ is the viscosity of air. The sample clamping plates in the DMPC have rectangular slots of length $L$ and width $W$. For the experiments with closures, the flow cross-sectional area is $A = L\delta$, where $\delta$ stands for the gap size in the closure, that is, the distance separating the two contacting surfaces constituting the closure. The pressure drop occurs across the overlap distance $l$ of the closure, because one edge of the closure is open to the top compartment of the DMPC whereas the other edge of the closure is open to the bottom compartment. Therefore, the pressure gradient driving the flow is $(-\partial P \partial Z) = \Delta P/l$ and Darcy's law can be rewritten as

$$k_D = \frac{\left(\frac{Q}{L\delta}\right)\mu}{\left(\frac{\Delta P}{l}\right)}$$

Recognizing that it is not easy to measure an unambiguous thickness $\delta$ for the closure, we combine the unknown $\delta$ with the permeability constant $k_D$ to write

$$\frac{1}{\delta k_D} = \frac{\Delta P L}{Q \mu l} = R_D$$

where we use $R_D$ to denote the measure of resistance to air permeation of the closure. From a practical point of view, we are really interested mainly in the ratio $\Delta P/Q$ because hermetic sealing requires increasing this ratio in order to reduce leakage rate $Q$ at any reasonable pressure drop. Note that all the remaining variables $L$, $l$, and $\mu$ are constants in the experiments done, with $L = 0.0254$ m, $l = 0.0127$ m, and $\mu = 1.79 \times 10^{-5}$ kg/(m s).

In our experiments, the volumetric flow rate $Q_{Bo}$ at the bottom outlet is measured as a function of the pressure drop $\Delta P$ maintained across the closure. The ratio $Q/\Delta P$ is constant for most of the cases, over the pressure drop investigated, that is, the air flow resistance is a constant independent of the pressure drop. Therefore, $Q/\Delta P$ can be estimated from the slope of the experimental $Q_{Bo}$ vs $\Delta P$ data.

$$\frac{Q}{\Delta P} = \frac{Q_{Bo2} - Q_{Bo2}}{\Delta P_2 - \Delta P_1}$$

where 1 and 2 refer to two different pressure drop conditions. For a few closure test samples, the applied pressure differential forces the two surfaces of the closure to open up, making the closure more air permeable, reflected by a change in slope (in the $Q$ vs $\Delta P$ plot) to larger values in some range of $\Delta P$. In those cases, we take the larger slope and only report the correspondingly smaller airflow resistance value.

## RESULTS AND DISCUSSION

**Roughness Measurements with AFM.** The properties of PSS/PAH polyelectrolyte multilayers used in this work have been investigated in a number of studies, comprehensively reviewed by Klitzing.[12] It is found that the thickness of PSS/PAH multilayers increases linearly with the number of deposition cycles. Neutron reflectivity studies show that the thickness of a bilayer (PSS/PAH) varies linearly with the ionic strength of the dipping solutions in the concentration range 0.5−3 M NaCl. With increasing salt concentration the multilayer growth with layer number becomes nonlinear, and the amount of adsorbed polymer increases more rapidly than linearly with the number of deposition cycles. For flexible polyelectrolytes like PAH and PSS, the resulting rms-roughness of the internal interfaces is of the order of the thickness of a single layer (approximately 2 nm). The outer layer roughness and internal interface roughness can be tuned by the preparation conditions. Both increasing ionic strength and increasing temperature during preparation leads to a larger internal roughness. However, there are no available data on the roughness and film thickness of PSS/PAH multilayers prepared using different salt solutions.

The films prepared from PEI(PSS/PAH) with different deposition number, salt type and concentration have rms outer surface roughness values in the range 3−7 nm (Table 1) with a standard deviation of about 2 nm. The roughness was analyzed on at least two independent multilayer samples with 5 equally divided areas on each. The roughness values measured at the 10 areas were averaged to provide the results in Table 1 along with the standard deviation values. The rms roughness values decreased in many cases (but not for all) when the number of bilayers was increased from PEI($PSS_5$/$PAH_5$) to PEI($PSS_{10}$/$PAH_{10}$). Although there are some variations in the roughness of the polyelectrolyte multilayers depending on their preparation conditions, the extent of this variation is much smaller than the variation we observed in the airflow resistance as discussed below. The slightly larger roughness observed under higher ionic strengths in most cases is in agreement with the qualitative trend reported in the literature.[12]

**Table 1. Roughness (in nm) of PEI-(PSS/PAH) Multilayers As a Function of the Electrolyte Type and Ionic Strength Used to Prepare the Polyelectrolyte Multilayers on PET Film As Substrate**[a]

| | 0.5 M NaF | 0.5 M NaCl | 0.5 M NaBr | 1.0 M NaF | 1.0 M NaCl | 1.0 M NaBr |
|---|---|---|---|---|---|---|
| | | | PEI-($PSS_5PAH_5$) | | | |
| root mean square (rms) avg | 5.01 | 5.53 | 4.55 | 8.50 | 6.09 | 5.39 |
| std. dev. | 1.69 | 1.73 | 1.73 | 1.92 | 2.89 | 2.41 |
| | | | PEI-($PSS_{10}PAH_{10}$) | | | |
| root mean square (rms) avg | 6.74 | 3.48 | 4.40 | 2.97 | 3.64 | 7.34 |
| std. dev. | 3.02 | 1.21 | 2.22 | 1.20 | 1.74 | 2.22 |

[a]The roughness was analyzed on at least two independent multilayer samples with 5 equally divided areas on each. The roughness values measured at the 10 areas were averaged to provide the tabulated results along with the standard deviation values.

**Adhesion Force Measurements with Colloidal Probe AFM.** The adhesive interactions between all PAH-terminated multilayers and the three different types of colloidal probes were measured using the AFM in air with approximately 45% relative humidity. One single sharp peak in the force−distance curve was observed for each type of probe interactions. In general, the adhesion forces obtained with a PSS functionalized colloidal probe were the largest while those measured with the COOH functionalized probe were the smallest. The interactions against the bare silica probe gave intermediate adhesion force values. The adhesion force distribution for the three types of probes is compared in Figure 4. Very narrow adhesion force distribution at around 70 nN was seen for a COOH functionalized probe. Relatively broader distribution was obtained for both the bare probe and the PSS functionalized probe. As mentioned previously, 25 or 50 force measurements were collected for each sample in air (five or ten different locations on the sample in both $x$ and $y$ directions, and five measurements were collected from each location) and the histogram in Figure 4 was constructed using a bin size of 50 nN.

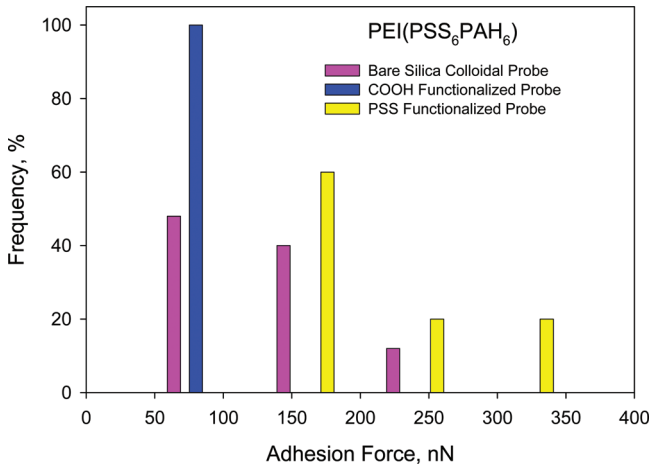


**Figure 4.** Probe effect on the adhesion force distribution for PEI ($PSS_6PAH_6$) multilayer. The adhesion force measured by bare silica colloidal probe, colloidal probe functionalized with COOH and the colloidal probe functionalized with a coated layer of PSS are shown. The multilayer with PAH as the outermost layer was prepared on plasma treated PET substrate, from polyelectrolyte solutions containing 0.5 M NaCl The force measurements were collected at 45% RH. The cantilever was moved to five different locations on the sample in both x and y directions, and five measurements were collected from each location, for a total of 25 force curves. The histogram is constructed using a bin size of 50 nN.

The AFM adhesion force between the polyelectrolyte multilayers prepared under different conditions of ionic strength and salt type with the PAH outermost layer against the COOH functionalized colloidal probe is shown in Figure 5. Both the average adhesion force based on 25 measurements and te standard deviation are shown for multilayers with either 5 or 10 bilayers. Adhesion forces in the range of 100 to 500 nN are obtained revealing some variations due to the type of salt, salt concentration and the number of layers. However, it is not possible to identify any systematic dependence of the adhesion strength on the variables investigated, from these data. We anticipate that the adhesion force of the multilayer closure (between one surface ending in PAH and the other surface ending in PSS) will be comparable to that measured between the multilayer ending in PAH and the PSS functionalized colloidal probe. Noting from Figure 4 that the adhesion strength against the COOH functionalized probe is about 3 to

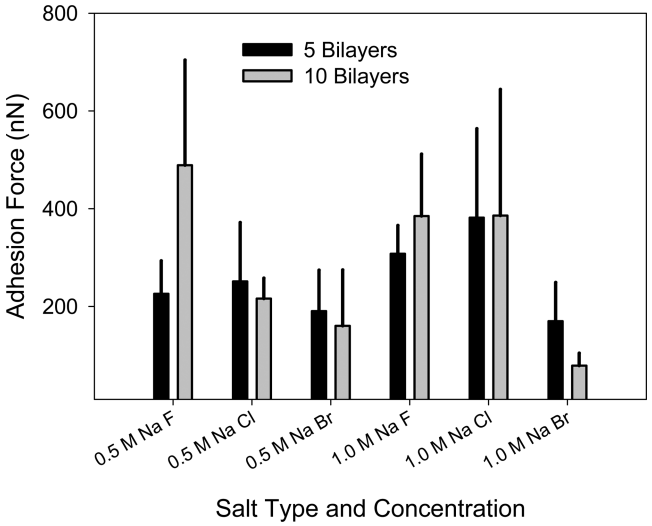


**Figure 5.** Dependence of average adhesion force determined from AFM measurements using a colloidal probe functionalized with COOH on electrolyte type and concentration used for multilayer preparation. The polyelectrolyte multilayer surface interacting with the colloidal probe had PAH as the outermost layer in all cases. The multilayer was prepared on plasma-treated PET substrate. The force measurements were collected at 45% RH. The cantilever was moved to ten different locations on the sample in both $x$ and $y$ directions, and five measurements were collected from each location. The reported average adhesion force and the standard deviation are based on these 50 measurements.

4 times smaller than that against the PSS functionalized probe, we estimate that the AFM adhesion force F between the multilayer and the PSS functionalized probe can be as large as 500 to 2000 nN (depending on the type of the polyelectrolyte multilayers, the ionic strength and the type of counterions utilized during the buildup of the multilayers and the number of layers in the multilayer system). The AFM force $F$ measured between a sphere (colloidal probe) of radius $R$ and a flat substrate (polyelectrolyte multilayer surface) can be related to the adhesive free energy per unit area W between two parallel planes by the Derjaguin approximation,[21] $F = 2\pi RW$. Accounting for the 1 $\mu$m diameter of the AFM colloid probe used (radius $R = 0.5$ $\mu$m), the measured AFM adhesion force F in the range 500 to 2000 nN between the flat multilayer and the spherical colloidal probe would correspond to macroscopic adhesion energies ($F/2\pi R$) in the range 0.16 to 0.64 N/m (or J/m$^2$) . For comparison, for the hook and loop mechanical closures utilized by the Army (uniforms and equipage), the peel strengths are required to be 0.5−1 lbs/inch (which translates into macroscopic adhesion energies of 90 to 180 N/m) depending on the type and class of the hook and loop. Therefore, the adhesion strengths of the multilayer closures are quite small compared to the mechanical hook and loop closures (such as Velcro) specified for Army applications.

**Airflow Resistance of Velcro Closure.** Velcro represents the most common closure in use. In the case of Velcro, permeation of gases can take place both through the closure region and through the surface of the Velcro, depending on what substrate the Velcro is attached. Indeed, the air permeation through the surface can be very significant even overwhelming the permeation through the closure region. To determine the airflow resistance of the Velcro closure region alone unaffected by the backup surface, we taped the back of the Velcro so that flow through the surface can be practically eliminated and only the flow through the closure will be measured. The results are shown in Figure 6, from which the

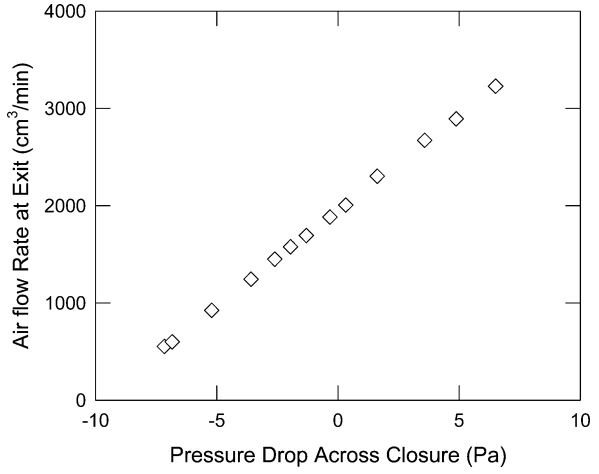


**Figure 6.** Experimental air flow results obtained from the DMPC showing the dependence of the flow rate as a function of the pressure drop for the Velcro closure with back of Velcro taped. Note the large slope and the small range of pressures accessible.

resistance to airflow for the Velcro closure is estimated to be $R_D = 0.053 \times 10^{12}$ m$^{-3}$. As mentioned above, the resistance of the Velcro closure would have been even smaller had we not taped the back of the Velcro to eliminate additional gas permeation pathways.

**Airflow Resistance of Polyelectrolyte Multilayer Closures.** Typical experimental measurements for the polyelectrolyte multilayer closure tested at 5, 25, 50, and 95% relative humidity values are shown in Figure 7. The results are

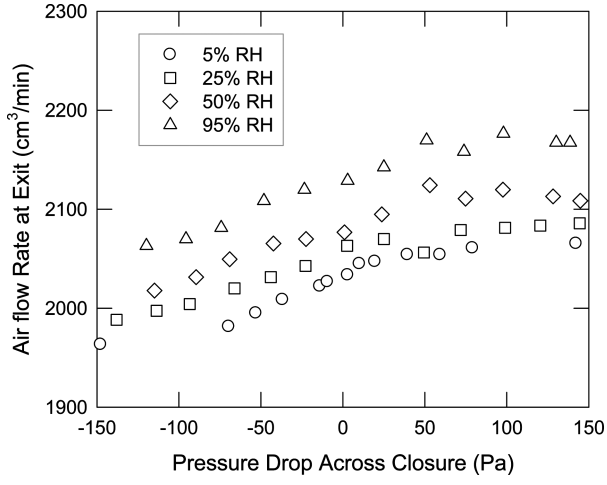


**Figure 7.** DMPC results for a typical polyelectrolyte multilayer closure system. The results are for the system PEI-(PSS5/6-PAH5) prepared with 1.0 M NaBr on PET substrate. Note the small slope and the wide range of pressure accessible.

for the system PEI-(PSS5/6-PAH5) prepared with 1.0 M NaBr on PET substrate. At all relative humidity values, the air flow resistances of the polyelectrolyte multilayer closure samples are much larger than those of the Velcro closure. The estimated airflow resistances of a number of polyelectrolyte multilayers are given in Table 2. It is difficult to discern a systematic


dx.doi.org/10.1021/am201784c | ACS Appl. Mater. Interfaces 2012, 4, 1620−1628

**Table 2. Dependence of Airflow Resistance of Polyelectrolyte Multilayer Closures on the Number of Layers and the Multilayer Preparation Conditions of Electrolyte Type and Ionic Strength[a]**

| overlapping multilayer closures | electrolyte concentration | pH of PSS/PAH dipping solutions | airflow resistance ($m^{-3}$) at specified relative humidity (RH) $\times 10^{12}$ 5% | 25% | 50% | 95% |
|---|---|---|---|---|---|---|
| PEI-PSS5/6-PAH5 | 0.5 M NaF | 9.12/7.19 | 1.9 | 1.5 | 1.3 | 0.9 |
| PEI-PSS10/11-PAH10 | 0.5 M NaF | 9.1/27.19 | 3.3 | 2.1 | 1.2 | 0.6 |
| PEI-PSS5/6-PAH5 | 1 M NaF | 9.43/7.41 | 22.6 | 29.2 | 22.0 | 10.5 |
| PEI-PSS10/11-PAH10 | 1 M NaF | 9.43/7.41 | 2.8 | 3.5 | 2.8 | 2.6 |
| PEI-PSS5/6-PAH5 | 0.5 M NaBr | 6.57/5.59 | 4.1 | 3.8 | 2.1 | 2.5 |
| PEI-PSS10/11-PAH10 | 0.5 M NaBr | 6.57/5.59 | 2.4 | 3.6 | 2.3 | 1.9 |
| PEI-PSS5/6-PAH5 | 1 M NaBr | 6.32/5.32 | 14.3 | 16.9 | 15.1 | 13.4 |
| PEI-PSS10/11-PAH10 | 1 M NaBr | 6.32/5.32 | 6.6 | 7.3 | 4.1 | 10.0 |
| PEI-PSS6-PAH5/6 | 0.5 M NaCl | 6.15/5.94 | 0.5 | 0.6 | 0.5 | 0.3 |
| PEI-PSS10/11-PAH10 | 0.5 M NaCl | 6.15/5.94 | 4.2 | 4.3 | 4.1 | 2.5 |
| PEI-PSS5/6-PAH5 | 1 M NaCl | 6.17/5.97 | 23.1 | 39.8 | 15.8 | 24.2 |
| PEI-PSS10/11-PAH10 | 1 M NaCl | 6.17/5.97 | 1.4 | 1.5 | 1.1 | 13.1 |

[a]The designation PEI-PSS5/6-PAH5 for a closure represents a system of two multilayer surfaces, of which one is PEI-$PSS_5$–$PAH_5$, with PAH as the outermost layer and the other is PEI-$PSS_6$–$PAH_5$, with PSS as the outermost layer.

variation in the airflow resistance as a function of the variables involved in the multilayer formation. From the expression for airflow resistance $R_D$ given for closures, we note that it depends on the closure thickness $\delta$ and the intrinsic permeation coefficient $k_D$. Therefore, one could anticipate that the resistance may decrease with an increase in the number of layers, because that would correspond to an increase in the closure thickness $\delta$. Although this trend is seen for a number of samples, the decrease in resistance is by an order of magnitude, whereas the number of layers increased by only a factor of 2. The multilayers prepared under these conditions showed comparable roughness values (Table 1). Therefore, surface conformational changes of the adsorbed polyelectrolyte layers may not account for the variations in the airflow resistance observed. The variations may be due to changes in the intrinsic permeation coefficient $k_D$ as a result of the differences in the nature of polyelectrolyte assembly under the differing preparation conditions.

We also measured the airflow resistance of a closure made of two overlapping PET films without any polyelectrolyte layers deposited on them. The PET films adhere to one another as can be expected and show an air flow resistance of $1.12 \times 10^{12}$ $m^{-3}$. Compared to this value, the presence of polyelectrolyte multilayers causes an additional increase in resistance as much as by a factor of 40.

**Effect of pH during Multilayer Preparation on Airflow Resistance.** The pH conditions during the preparation of the polyelectrolyte multilayer may control the extent of ionization of one or the other polyelectrolyte involved and thereby influence how the assembly and conformation of the alternating layers occurs. If the polyelectrolyte is more strongly ionized, it may bind to the preceding polyelectrolyte layer more tightly and the resulting closure system may be a less porous system from the point of view of air permeation. The airflow resistances estimated at two values of pH are shown in Table 3 for the systems PEI-(PAH5-6-PSS5) and

PEI-(PAH11/10-PSS10) is prepared with 0.5 M NaCl on PET substrate and from 1.0 M NaCl on PI substrate. Increasing pH mainly caused an increase in the airflow resistance, even though one system showed an exception. Increasing pH would decrease the ionization extent of PAH, which is a weak polyelectrolyte, whereas the ionization of the strong poly-

**Table 3. Dependence of Airflow Resistance of PEM Multilayer Closures on pH during Multilayer Preparation**

| overlapping multilayer closures | pH of PSS and PAH dipping solutions | airflow resistance ($m^{-3}$) at specified relative humidity (RH) $\times 10^{12}$ 5% | 25% | 50% | 95% |
|---|---|---|---|---|---|
| Substrate PET, 0.5 M NaCl | | | | | |
| PEI-PSS5-6-PAH5 | 3.5 | 7.4 | 5.4 | 3.2 | 8.6 |
| PEI-PSS10/11-PAH10 | 3.5 | 6.1 | 4.2 | 2.4 | 1.4 |
| PEI-PSS5/6-PAH5 | 7.5 | 20.0 | 17.8 | 14.5 | 9.3 |
| PEI-PSS10/11-PAH10 | 7.5 | 6.7 | 5.0 | 3.0 | 1.8 |
| Substrate PI, 1.0 M NaCl | | | | | |
| PEI-PAH5-6-PSS5 | 3.5 | 11.7 | 8.5 | 1.5 | 0.6 |
| PEI-PAH11/10-PSS10 | 3.5 | 20.0 | 19.5 | 18.8 | 15.2 |
| PEI-PAH6/5-PSS5 | 7.5 | 11.2 | 12.6 | 5.6 | 1.0 |
| PEI-PAH11/10-PSS10 | 7.5 | 13.0 | 14.6 | 12.0 | 2.6 |

electrolyte PSS is expected to remain unaffected. The absence of tight binding between a highly ionized polyelectrolyte and a weakly ionized polyelectrolyte will lead to a more porous multilayer system resulting in a decreased airflow resistance. However, this expectation is in contrast to the experimental observation and therefore the airflow resistance is unlikely to be determined by the polymer confirmations within the closure region.

**Effect of Humidity on Airflow Resistance.** Experimental results presented in Tables 2 and 3 show either a small decrease or lack of change in the airflow resistance with increasing relative humidity, although there are some exceptions to this rule in the experimental data. Further, the change in airflow resistance with humidity is nonlinear with more appreciable variations at the higher relative humidity values. Previous studies by Wehner et al.[22] on textile materials showed that large airflow resistance changes are possible when humidity changes,

and mostly, the airflow resistance increased nonlinearly with increasing humidity. An explanation was offered by considering the textile material as a porous medium made up of the individual fibers, and recognizing that the increase in humidity would cause the swelling of fibers and thereby decrease the porosity of the textile and increase its airflow resistance. Later experiments by Gibson et al.[14] showed deviations from this behavior for nylon fabrics, which displayed a decrease in airflow resistance with increasing humidity. It was speculated that the nylon fibers may swell axially rather than radially, modifying the dependence of porosity on humidity in a very different manner. In both cases, whether airflow resistance increases or decreases, the significant change in airflow resistance was found to occur in the higher humidity region.

In the case of the polyelectrolyte multilayer closures, we do not have any phenomenon equivalent to that of fiber swelling. The multilayer is a molecular scale assembly and the incorporation of water due to humidity changes would cause the multilayers to possibly swell and the closure system will have a different gap thickness, thereby increasing the porosity of the closure in contrast to the behavior of common textile fibers where porosity decreases due to fiber swelling. Such a phenomenon is consistent with the observed decrease in the air flow resistance polyelectrolyte multilayer closures with increasing relative humidity.

**Interpreting Airflow Resistance in Terms of Closure Opening.** Intuitively, the airflow resistance can be expected to have a correlation against the roughness of the polyelectrolyte multilayer surface, since the surface roughness may be assumed to influence the porosity of the air flow region in the closure. Similarly, the airflow resistance can be expected to be correlated against the adhesion force between the multilayers since stronger adhesion can be expected to keep the closure layers together when a pressure gradient is applied. In Figure 8, the

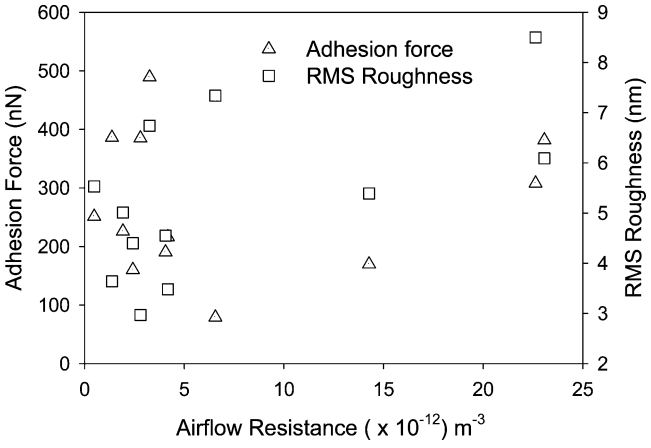


**Figure 8.** Correlation of air flow resistance measured by the DMPC to adhesion force and rms roughness measured by AFM for the systems PEI-(PSS5/6-PAH5) and PEI-(PSS10/11-PAH10). The polyelectrolyte systems prepared in 0.5 and 1.0 M solutions of different salts are defined in Table 2.

measured airflow resistance is correlated against the adhesion force measured using the colloidal probe functionalized with COOH and also against the root-mean-square (rms) roughness of the multilayer surface, measured by the AFM. The data in Figure 8 suggest no direct relationship between the airflow resistance and the adhesion force or the rms roughness of the multilayer outer surface.

To understand the absence of any such correlation, we can investigate what may be the flow region of air. We can develop a rough estimate of the air flow area assuming viscous flow of air through the closure. Treating the closure opening as a rectangular slit between two parallel surfaces of width $L$ and slit opening $d$, the airflow rate under laminar flow conditions can be written as

$$Q = \left(\frac{\Delta P}{l}\right)\frac{Ld^3}{12\mu}$$

Combining this expression with the expression given earlier for the airflow resistance $R_D$, the slit opening d can be calculated as

$$d = \left(\frac{12}{R_D}\right)^{1/3}$$

For the airflow resistances $R_D$ in the range $1-40 \times 10^{12}$ $m^{-3}$ listed on Tables 2 and 3, this would yield a slit opening of $d$ in the range 230 to 65 $\mu$m. The Reynolds number for flow through the slit can be calculated as

$$Re = \frac{\rho V d}{\mu} = \frac{\rho Q}{L\mu}$$

and the resulting low values for the Reynolds numbers justify the use of the laminar flow equation. These rough estimates for the slit thickness (or closure opening) are much larger than the expected multilayer thickness (of the order of 20−40 nm) and the surface roughness. This suggests that when an applied pressure differential is applied over the closure, the two surfaces constituting the closure can be moved from one another to create microscopic gaps between surfaces of the order of 10s to 100s of $\mu$m. The airflow resistance appears to be controlled by the significant inter layer separation occurring as a result of the applied pressure differential; the resistance has no obvious correlation against various properties of the multilayers such as multilayer thickness, surface roughness, or adhesion between the layers. It is quite possible that the extent of this displacement between the closure layers is influenced by the adhesion between the layers, which in turn is affected by the surface roughness. However, this connection is not direct and remains to be established.

## CONCLUSIONS

Polyelectrolyte multilayer closures explored in this study based on a single polyelectrolyte pair provide airflow resistance (measured by the parameter $R_D$) in the range 1 to $40 \times 10^{12}$ $m^{-3}$ which is roughly 20−800 times larger than that provided by the Velcro type mechanical hook and loop closures ($0.053 \times 10^{12}$ $m^{-3}$). Indeed, this estimate for the airflow resistance for the Velcro type closure is an upper bound because the permeation through only the closure region was measured by taping the back of the Velcro; the permeation resistance of Velcro closure as it is usually attached to clothing surfaces would be even smaller. The air flow resistance of the polymer multilayer closure generally decreases with increasing relative humidity, but for some multilayer preparations this decrease is minimal. The ionic strength, type of counterion, and pH at which the multilayers are prepared, as well as the number of layers in the multilayer, all have some influence over the airflow resistance, though no systematic dependencies could be quantitatively determined. An analysis of flow through the system suggests that when an applied pressure differential is

applied over the closure, the two surfaces constituting the closure are moved from one another to create microscopic gaps between surfaces of the order of 100s of $\mu$m. The airflow resistance appears to be controlled by the significant inter layer separation occurring as a result of the applied pressure differential. The resistance has no obvious correlation against various properties of the multilayers such as multilayer thickness, surface roughness or adhesion between the layers. The results do suggest that from the point of view of providing a good seal against toxic gas permeation, the polymer multilayers are interesting candidates for closure systems. Since the adhesion strength of the multilayer closures estimated based on AFM measurements are quite small compared to those of mechanical closures specified for Army applications, it would be necessary to engineer a composite closure system combining the mechanical closure to provide strong adhesion and the multilayer closure to provide hermetic sealing.

## AUTHOR INFORMATION

### Corresponding Author

*Phone: 508-233-6445. Fax: 508-233-4469. E-mail: Ramanathan.Nagarajan@us.army.mil.

### Notes

The authors declare no competing financial interest.

## ACKNOWLEDGMENTS

Work was supported by the Defense Threat Reduction Agency (DTRA) Project BA08PRO021.

## REFERENCES

(1) Autumn, K.; Sitti, M.; Liang, Y. A.; Peattie, A. M.; Hansen, W. R.; Sponberg, S.; Kenny, T. W.; Fearing, R.; Israelachvili, J. N.; Full, R. J. *Proc. Natl. Acad. Sci. U.S.A.* **2002**, *99*, 12252.
(2) Arzt, E. *Mater. Sci. Eng., C* **2006**, *26*, 1245.
(3) Tian, Y.; Pesika, N.; Zeng, H.; Rosenberg, K.; Zhao, B.; McGuinnen, P.; Autumn, K.; Israelachvili, J. N. *Proc. Natl. Acad. Sci. U.S.A.* **2006**, *103*, 19320.
(4) Decher, G. *Science* **1997**, *277*, 1232.
(5) Schlenoff, J. B.; Dubas, S. T.; Farhat, T. *Langmuir* **2000**, *16*, 9968.
(6) Izquierdo, A.; Ono, S. S.; Voegel, J. C.; Schaaf, P.; Decher, G. *Langmuir* **2005**, *21*, 7558.
(7) Krogman, K. C.; Zacharia, N. S.; Schroeder, S.; Hammond, P. T. *Langmuir* **2007**, *23*, 3137.
(8) Félix, O.; Zheng, Z.; Cousin, F.; Decher, G. *C. R. Chim.* **2009**, *12*, 225.
(9) Fukao, N.; Kyung, K. H.; Fujimoto, K.; Shiratori, S. *Macromolecules* **2011**, *44*, 2964.
(10) Delcorte, A.; Bertrand, P.; Wischerhoff, E.; Laschewsky, A. *Langmuir* **1997**, *13*, 5125.
(11) Chen, W.; McCarthy, T. J. *Macromolecules* **1997**, *30*, 78.
(12) Klitzing, R. v. *Phys. Chem. Chem. Phys.* **2006**, *8*, 5012.
(13) Gibson, P.; Rivin, D.; Cyrus, K. *Convection/Diffusion Test Method for Porous Materials Using the Dynamic Moisture Permeation cell*; Natick Technical Report; Natick/TR-98/014 ; Natick Soldier Center: Natick, MA, 1997.
(14) Gibson, P.; Rivin, D.; Cyrus., K.; Schreuder-Gibson, H. *Text Res. J.* **1999**, *69*, 311.
(15) Claesson, P. M.; Dedinaite, A.; Rojas, O. J. *Adv. Colloid Interface Sci.* **2003**, *104*, 53.
(16) Mermut, O.; Lefebvre, J.; Gray, D. G.; Barrett, C. J. *Macromolecules* **2003**, *36*, 8819.
(17) Bosio, V.; Dubreuil, F.; Bogdanovic, G.; Fery, A. *Colloids Surf., A* **2004**, *243*, 147.
(18) Gong, H.; Garcia-Turiel, J.; Vasilev, K.; Vinogradova, O. I. *Langmuir* **2005**, *21*, 7545.
(19) Notley, S. M.; Eriksson, M.; Wagberg, L. *J. Colloid Interface Sci.* **2005**, *292*, 29.
(20) Johansson, E.; Blomberg, E.; Lingstrom, R.; Wagberg, L. *Langmuir* **2009**, *25*, 2887.
(21) Israelachvili, J. N. *Intermolecular and Surface Forces*, 2nd ed.; Academic Press, San Diego, 1991; Chapter 10.
(22) Wehner, J. A.; Miller, B.; Rebenfeld, L. *Text Res. J.* **1987**, *57*, 247.